

Automatic Building of Structured Geological Models

Sylvain Brandel¹, Sébastien Schneider², Michel Perrin³, Nicolas Guiard³, Jean-François Rainaud², Pascal Lienhardt⁴ and Yves Bertrand⁴

¹ Université Louis-Pasteur, LSIT, Pôle API, Bd Sébastien Brant, F-67400 Illkirch
brandel@lsiit.u-strasbg.fr

² Institut Français du Pétrole, DISMA, 1-4 Avenue de Bois-Préau, F-92852 Rueil-Malmaison Cedex
{sebastien.schneider,j-francois.rainaud}@ifp.fr

³ Ecole des Mines de Paris, CGI, 60 Bd St. Michel, F-75272 Paris Cedex 06
{perrin,guiard}@cge.ensmp.fr

⁴ Université de Poitiers, IRCOM-SIC, Bat. SP2MI, Téléport 2, Bd Marie et Pierre Curie, BP 30179, F-86960 Futuroscope Cedex
{lienhardt,bertrand}@sic.sp2mi.univ-poitiers.fr

Abstract

The present article proposes a method to significantly improve the construction and updating of 3D geological models used for oil and gas exploration. The proposed method takes advantage of the specific structures which characterize geological objects. We present a prototype of a “geological pilot” which enables monitoring the automatic building of a 3D model topologically and geologically consistent, starting from a set of unsegmented surfaces. The geological pilot uses a “Geological Evolution Scheme” (GES) which records all the interpretation elements that the exploration geologist, who is the end user, wishes to introduce into the model. The model building is performed by reading instructions deduced from the GES. Topology is dealt with step by step by using a “3D Generalized Maps” (3-G-Maps) data model enriched to enable the manipulation of objects having specific geological attributes. The result is a correct 3D model on which geological links between objects can easily be visualized. This model can automatically be revised in case of changes in the geometric data or in the interpretation. In its final version, the created modular tool will be plugged in 3D modelers currently used in exploration geology in order to improve their performance.

Categories and Subject Descriptors (according to ACM CCS): I.3.5 [Computer Graphics]: Computational Geometry and Object Modeling

1. Introduction

Different types of 3D modelers are available for research and geological exploration [FHHR98] [Mal92] [webf] [webc]. There exist major differences between them related to the type of surface representation chosen generally triangular (GOCAD [Mal89] [Mal92] [Mal02] [webe]) or parametric (RML [FHHR98] [weba]), the method used for assembling them either manually or in a semi-automatic way, and to the quality of the final result, which may be a topologically consistent 3D model or a mere assemblage of surfaces. Generally speaking, geological 3D models must comprise very numerous data and often have a large size. For this reason, their building often requires important computing times and their revision, in case of data or interpretation changes, is generally a delicate and lengthy operation.

The aim of the present paper is to achieve significant improvements to 3D geological modeling by taking advantage of the specific structure which underlies consistent geological assemblages.

Geometrically, a 3D geological model consists of a set of elementary volumes (geological blocks), each fully bounded by surfaces, the global topology being that of a 3D jigsaw puzzle with

no voids. However, the main peculiarity of underground models is due to the fact that the assemblage represents a given “geology” which records the evolution of underground through geological ages [HMW76]. Specific processes took place during various spans of time, generally millions of years, inducing creation, destruction or transformation of matter. Each definite surface of the model is the record of one remarkable geological event, which can be considered as having been instantaneous with respect to the geological time scale. Consequently, before building a model, the geologist *interprets* the “geology” to be represented by establishing between the various surfaces a **total or partial order relationship based on chronology** (cf. Figure 1.a). Specific links also exist between geological blocks. Each block is made of matter created during a definite span of time and thus belongs to a definite geological formation (cf. Figure 1.b).

The geological nature of the model influences its geometry. For instance, since geological surfaces limit volumes occupied by solid matter, **two geological surfaces cannot cross each other**. For this reason, a geological model will only be consistent if surface crossings always consist in one surface interrupting the other with no possible X-crossings.

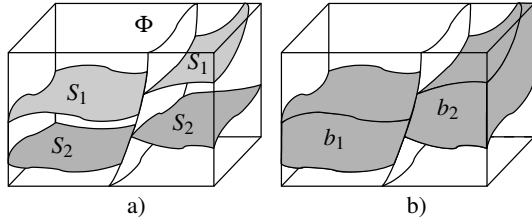


Figure 1: a) S_1 and S_2 are two geological surfaces (S_1 younger than S_2) intersected by a later fault ϕ . b) b_1 and b_2 are two geological blocks between S_1 and S_2 , which belong to one formation.

The 3D models provided by current geological modelers do not always specify the age relationships existing between the various volumes and surfaces that they represent. Worse, they may sometimes be geologically inconsistent, displaying for instance intersections that cannot be correct in view of the ages of the surfaces involved.

Our opinion is that the specific structure of geological assemblages, far from being a difficulty, can, on the contrary, facilitate their construction.

We will demonstrate that it is possible to take advantage of the specificity of geological structures to pilot the automatic building of a 3D consistent geological model. The various geological surfaces will be put into place one after another taking into account their relative chronological order and the necessary intersections will be operated at each step. For this, we propose to add to the current 3D geological modelers, **a geological pilot**. This pilot enables production of models of better quality, which are fully consistent both topologically and geologically and which can be built and updated in a fully automatic way.

The pilot prototype presented here operates two functions, which do not exist in classical 3D geological modelers:

- the recording of all the geological relationships that the end user wishes to put in the model in a “**Geological Evolution Scheme**” (GES) (cf. Section 2.1.2);
- an automatic building of the model, surface after surface, according to instructions read on GES (cf. Section 3).

3D geological models are “true” 3D models, since they deal not only with surfaces but with actual volumes. For this reason, the building of the model necessitates the use of a data structure that enables dealing with 3D topologies and adequate operators for intersecting and assembling 3D surfaces and volumes. Specific tools must also be added so that the representation of specific entities such as geological formations can be represented. We will use here **extended 3-G-Maps** [Lie89] [Lie94] which enable the manipulation of geological objects.

GES and 3-G-Maps are generic tools. They will be used here in the frame of a specific modeler RML/GeoSurf [FHHR98] developed by IFP/BEICIP [weba]. The main characteristic of RML is the use of 3D trimmed parametric surfaces. Extended G-Maps enable defining the intersections that must be operated at each stage of the model building and to generate a topologically and geologically consistent result. The result is an “intelligent” model in which any geological element can be localized and visualized in 1D, 2D or 3D.

We will first present the main tools which will be used: the geological syntax rules on which the modeling is based, the G-Maps data model and the 3D modeler GeoSurf, a module of the Reservoir Modeling Line (RML) in which our prototype is inserted. We will then present the model building process. A few significant results will be presented and discussed. We will finally consider the future development of the proposed methodology and conclude.

2. Theoretical and practical background

2.1. Geological syntax and Geological Evolution Scheme (GES)

2.1.1. Geological syntax

Previous work [Per98] has shown that, in order to be geologically consistent, 3D models should be built in accordance with a few rules, which define a **geological syntax**.

We assume that surfaces present in a 3D model are of two types (cf. Figure 2):

- **polarized surfaces (POL)** consisting in limits of sedimentary formations corresponding to former sea bottoms or to limits of former molten rocks corresponding to intrusive granites; in these cases, the two surface sides are geologically different: one facing older formations (= F-old) and the other faces younger formations (= F-young);
- **non polarized tectonic surfaces (TEC)** which correspond to geological discontinuities, faults for instance, whose two faces are geologically equivalent both facing older formations.

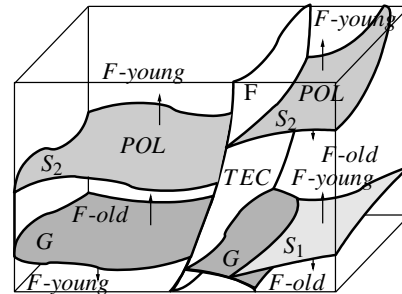


Figure 2: POL and TEC surfaces. S_1 , S_2 sedimentary POL surfaces (upper side corresponds to F-young); G granite limit POL surface (upper side corresponds to F-old); F fault TEC surface.

The fundamental rules are that each surface, either POL or TEC, has **one** well-determined age and that, when two surfaces intersect, one of them is necessarily interrupted by the other.

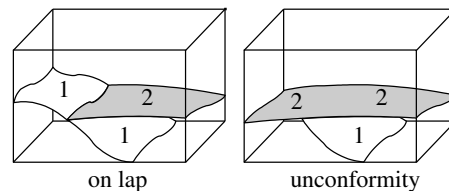


Figure 3: Two types of intersection between surfaces.

Space-time relationships between intersecting geological surfaces can be of two types (cf. Figure 3):

- *on lap*: when the older surface (1) is a POL (on lap surface), it interrupts the younger surface (2); intersection of (2) with a TEC is impossible;
- *unconformity*: the younger surface (unconformable surface 2) interrupts the older surface (1).

In order to deal with these cases in any geometric configuration, the F-old face (resp. F-young face) of each surface are given:

- the attribute conformable (CF) if they are, interrupted by all older (resp. younger) surfaces;
- the attribute unconformable (UC) if it interrupts all older (resp. younger) surfaces.

These attributes are given in the following way:

- default values: F-old, F-young = CF;
- on lap surface: F-young = UC;
- unconformable surface: F-old = UC.

following the rules on Figure 4 for intersecting surfaces.

		Younger Surface 2	
		F.old=CONC	F.old=DISC
Older Surface 1	F.young=CONC	IMPOSSIBLE	2 cuts 1 (unconformity)
	F.young=DISC	1 cuts 2 (on lap)	2 cuts 1 (unconformity)

Figure 4: Intersection rules for POL surfaces.

2.1.2. Geological Evolution Scheme (GES)

An *i*-order GES is a graph for which nodes are (cf. Figure 6):

- individual surfaces POL or TEC, whose faces have been given attributes CF/UC in accordance with the rules defined above (cf. Figure 4);
- an *i+1*-order GES, corresponding to an increased level of detail.

The nodes are put in vertical order in accordance with their relative age (bottom = old, top = young) and joined by various types of arcs (cf. Figure 5).

The GES is built by the user in view of his/her interpretation of the available geometric data. He/She creates nodes of the graph corresponding to various geological events and arcs which link these nodes according to chronology (a definite event is anterior/posterior to another) or to specific spatial relationships (a definite fault stops on another one) [BPRS01] (cf. Figure 5).

The root node of the GES corresponds to the limits of the scene (bounding box), which is considered as the youngest event (cf. Figure 6).

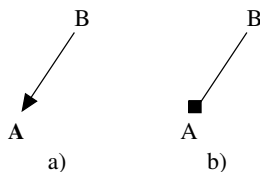


Figure 5: a) Event A is anterior (older) to event B; b) Fault A stops on fault B.

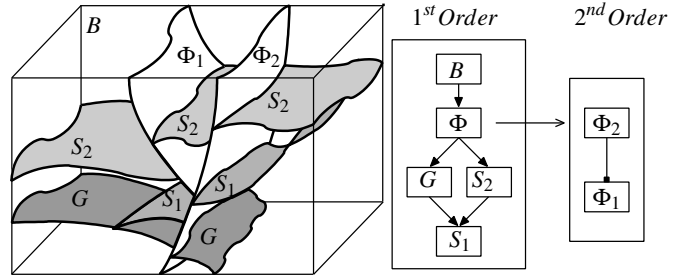


Figure 6: 1st and 2nd order GES associated to a geological scene.

2.2. Topological data model: Generalized Maps

2.2.1. Generalized Maps (G-Maps)

The 3D models that must be performed should be true “volumic models” which requires that they should be topologically consistent. This requires the use of a topological data model, which partitions an object into topological cells of different dimensions (vertices, edges, faces and volumes), and specifies the relations between them.

For example, a 2D object consisting in a triangle on the top of a square (cf. Figure 7.a) is described by a G-Map by decomposing it into two faces, which can in turn be decomposed in edges. The G-Map structure assumes that each edge consists in two *darts*, a *dart* being the atomic element of the data model. In dimension 2, a *dart* is the restriction of the vertex to a given edge and a given face (cf. Figure 7.a). A specific *dart* can be linked to other *darts* by means of *sews*, marked α_i ($0 \leq i \leq n$, where n is the dimension of the G-Map). An α_i *sew* links two *darts* which belong to two different *i*-cells (cf. Figure 7.b): in the case of a 3D model, α_0 links two vertices, α_1 links two edges, α_2 links two faces and α_3 links two volumes.

Specific cells of the G-Map can be identified by considering parts of the *sew* classes : vertices are obtained by omitting α_0 *sews* (cf. Figure 7.c), edges by omitting α_1 *sews* (cf. Figure 7.d), faces by omitting α_2 *sews* (cf. Figure 7.e) and volumes by omitting α_3 *sews*.

In order to describe a model, a G-Map should be *embedded* in a definite geometry. This is done by associating each geometrical element of a given dimension with a specific cell of the G-Map: for instance, in the 3D models considered here, surfaces can be associated with faces, curves with edges and points with vertices. Surfaces are trimmed patches defined by a parametric surface extent and by parametric curves corresponding to a restriction defined on the extent of the u, v domain.

The G-Map structure can be applied to describe a **macrotopology** i.e. the topological relationships existing between the various edges, faces, volumes of a 3D model described by a set of surfaces of any type (parametric, triangulated, meshed etc.). 3 types of embedding will then be used:

- vertex embedding related to 3D points;
- edge embedding related to 3D parametric curves or to polygonal lines;
- face embedding related to parametric, triangulated or meshed portions of surfaces.

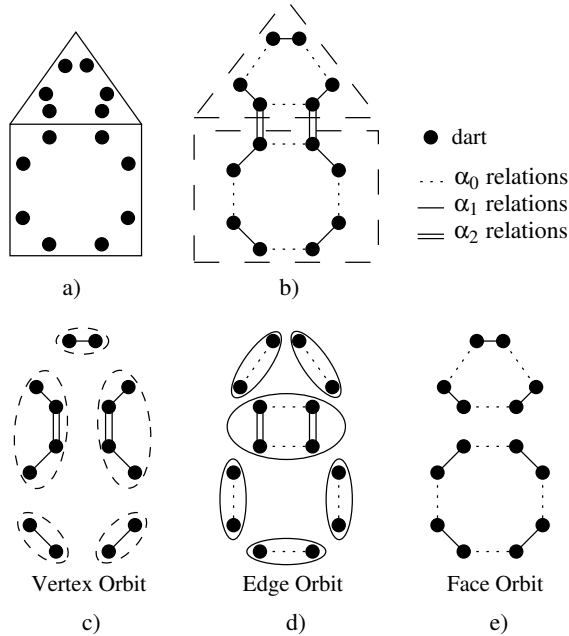


Figure 7: 2-G-Maps description: a) darts corresponding to geometric object; b) relations between darts; c) vertex orbit; d) edge orbit; e) face orbit.

In the case of a model consisting of triangulated or meshed surfaces, the G-Map structure can also be applied to describe the relationships between the various elementary edges and triangular or polyhedral surfaces (**microtopology**) (cf. Figure 8).

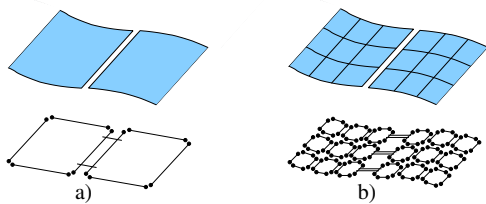


Figure 8: a) Macrotopological and b) microtopological description of a parametric surface divided in two patches.

2.2.2. Extension for describing geological relationships

Figure 9.b shows a 3D geological scene before interpretation. It consists of two independent surfaces G and T which correspond to 3-G-Maps (represented with 2-G-Maps on the figure) face embeddings and two GES nodes (cf. Figure 9.a). Each surface is associated to a face composed of two sides linked by α_3 sews (cf. Figure 10.a) (each curve corresponding to an edge composed of two sides linked by α_2 sews in 2D).

The GES shows that surface G should be cut by the T erosion surface. Intersection of G by T induces a division of G into three parts, one of which must be removed from the model. The 3-G-Map (the 2-G-Map on Figure 9.c) is accordingly modified and now consists of G_1 , G_2 and T_1 , T_2 , T_3 . However, G_1 , G_2 and T_1 , T_2 , T_3

respectively belong to only two geological surfaces G and T . Thus we have to put an extra β_2 link (β_1 in 2D) to emphasize the geological relation, which exists between discontinuous geometrical parts (cf. Figure 10.b).

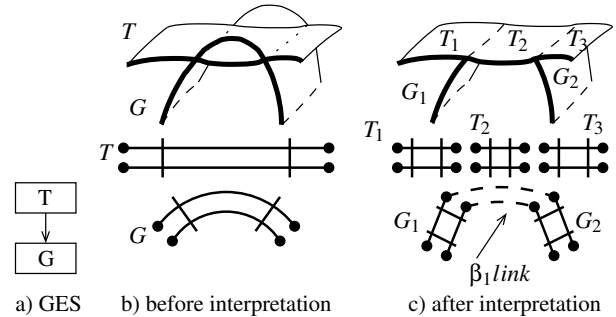


Figure 9: G-Maps extension to keep geological relationships, the 2-G-Map shown corresponding in fact to the bold curves topology on front side of the 3D geometric model.

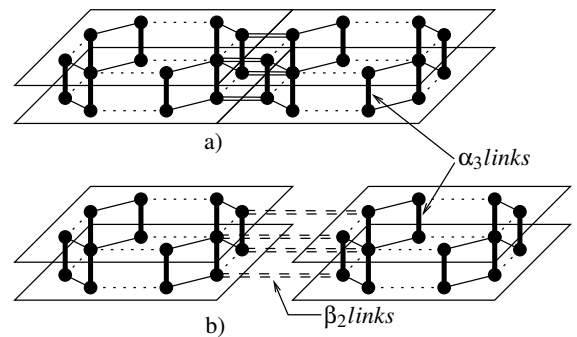


Figure 10: Extended 3-G-Maps description (vertical bold links representing α_3 sews between both sides of a face): a) two continuous geometric surfaces sewed with α_2 relations; b) two segmented geometric surfaces sewed with extended relations β_2 (double dashed links).

More generally, the different geological elements can be identified using the 3-G-Map cells: each geological surface is described by one or several faces linked by α_2 and β_2 relations, each 3D block by a volume of the 3-G-Map and each geological formation by one or several 3D blocks, whose linkage can be retrieved using POL geological surfaces, which face CF inside geological formation.

2.3. Geometric tools

The software object of this paper uses the following previously available geometric tools:

- a topological kernel from the Poitiers university, including the G-Map structure and the related operations [Lie89] [HH00] [BDFL93] [Lie94];
- the Reservoir Modeling Line (RML) developed by Institut Français du Pétrole (IFP). RML deals with 3D parametric surfaces, which are considered as extents; one or more restrictions are associated with each surface, each of them being defined in the u,v space of the extent; all operations related to surfaces are

operated on the restrictions and thus correspond to 2D operations.

RML uses a few features of CAS.CADE, a huge CAD library developed by MATRA-DATAVISION in 1993 [webb] to manage all geometrical operations involving parametric surfaces. This enables consideration of intensively deformed surfaces that can be in overlapping position, a common case in geology. Its main advantages are robustness and stability. Moreover, parametric surfaces enable dealing with uncertainties in a very flexible way. However, computing time can be rather long when high precision is required. CAS.CADE is now available in open source [webb].

G-Maps and CAS.CADE libraries are used together, CAS.CADE objects corresponding to the embedding of G-Maps objects.

3. Model building

3.1. Overall model building methodology

The overall methodology proposed here involves the four main following operations:

1. data input and GES building;
2. determination of the intersections to be performed;
3. fault preprocessing;
4. model building (involving at each stage surface intersection and removal of all undesired parts).

3.1.1. Data input and GES building

Initial surfaces are assumed to be continuous, unstructured and geometrically independent from one another, possible intersections between them being ignored.

The GES must be built by the user before the building of the model itself. For this, he/she must define the relative age order of the various geological surfaces and define the properties of each of them: POL or TEC and in the case of a POL surface, CF or UC. He/She also specifies the links between the various geological surfaces and the various files describing their geometries (cf. Figure 11).

For the moment, the above operations are executed manually. However, an independent user interface is presently being built and will allow to define the links and properties of the various geological surfaces, and to insert them in a GES that will be built automatically [BHB03].

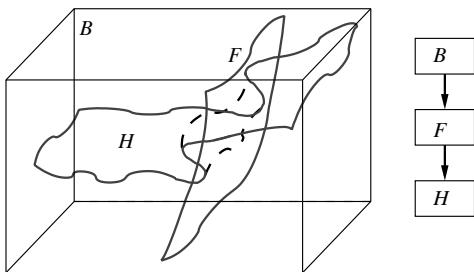


Figure 11: Data input: two unsegmented geological surfaces F and H and the corresponding GES. Each arrow goes from the younger surface to the older one.

3.1.2. Determination of the intersections to be operated

The partial order relationship established between the various geological surfaces by means of the GES is used to build a consistent model step by step. The rule is that an older geological event cannot modify a younger one. In consequence, the various geological surfaces must be introduced one after the other in reverse chronological order, beginning by the youngest one. Each geological surface is introduced by intersecting it with all the younger surfaces already present in the model.

In practice, the various intersections that must be operated are identified by running through the GES graph from top to bottom (interpretation course) and, for each node v_i met, from this very node to the top (intersection courses). The second course is launched if and only if all the ascendants of the current node v_i have already been interpreted. Otherwise, we recursively go back to process the upper following branch of the graph that has not already been interpreted (cf. Figure 12).

It results that, for each node v_i met during the intersection course, a couple of potentially intersecting surfaces is identified, which respectively correspond to an older geological surface n_i and to a younger one n_j , v_i being the current node of the intersection course.

It remains to determine which of the older surface n_i or of the younger one n_j interrupts the other. This is very easily done by retrieving from the GES the UC or CF properties of the relevant sides of n_i and n_j and by applying the rules given Figure 4.

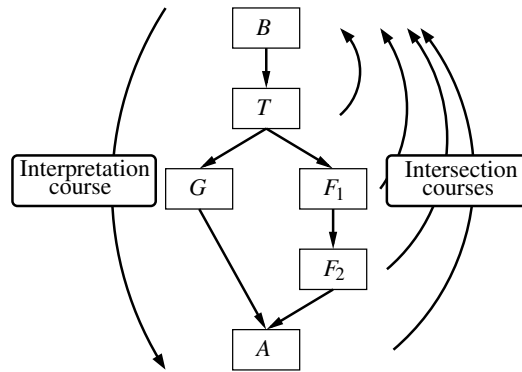


Figure 12: Determination of the intersections to compute by going through the GES with imbricated interpretation and intersection courses; for each step of the interpretation course, we run an intersection course.

3.1.3. Preprocessing

When intersecting locally subparallel surfaces, multiple intersections may appear that may merely be artifacts. This is notably the case when a fault induces an offset in the surfaces that it interrupts (cf. Figure 13).

In order to avoid this, we operate a preprocessing by building on both sides of the interrupting surface F two parallel surfaces F_1 and F_2 at a distance d chosen by the user in view of his/her estimation of the breadth of the uncertainty zone around the model. The volume comprised between F_1 and F_2 can then be considered as a blind volume in which the initial data concerning any interrupted

surface H can be considered as no longer valid. In practice, this may sometimes induce the splitting of H into different parts that must be sewn by β_2 topological relations in order to express that they are parts of one geological surface (cf. Figure 13).

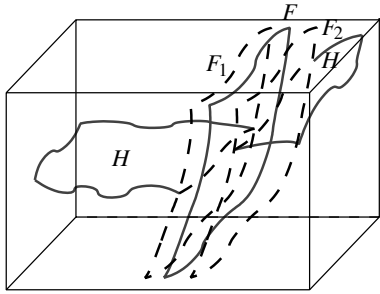


Figure 13: The preprocessing stage.

3.1.4. Model building

The model building has been undertaken by using two different methodologies.

A first method has been implemented starting from the parametric surfaces currently available in RML and considering a **macro-topological approach**. In this preliminary approach, we have considered that any new surface introduced into the model either stops on one or several previously introduced surfaces or entirely crosses the whole model. As will be seen in Section 4, this method can provide satisfactory results for models which only comprise major faults regularly stopping one on the other. Conversely, this technology cannot be used for building models, which comprise “hanging faults” (which stop inside definite blocks) or faults of minor extension.

This is the reason why we are presently developing a second methodology based on the **co-refinement** of triangulated surfaces described by the mean of their **microtopologies** [CD96b] [CD96a]. This methodology is in course of implementation, but already provides promising results.

3.2. Method using a macrotopological approach

This method has been developed by Sébastien Schneider and Sylvain Brandel at Ecole des Mines de Paris and University of Strasbourg [BPRS01] [Sch02]. It considers surfaces defined according to the CAS.CADE format: parametric extent surface and restriction curves. We suppose that each CAS.CADE surface corresponds to one geological surface (cf. Figure 14).

The methodology assumes six stages for the building of the model, which are illustrated on the elementary model shown on Figure 14:

1. we initially consider the set of all the surfaces to be assembled (F and H in the example, F being a fault and H a polarized geologic surface) (cf. Figure 14.b) and the corresponding GES (cf. Figure 14.a);
2. we perform a preprocessing in order to avoid uncertainties concerning intersections between faults (F) and polarized surfaces (H); it involves fault thickening and a segmentation of the polarized surfaces, which consists in deleting all the parts of

H located within the uncertainty zone built around F (cf. Figure 14.c).

The model is then built step by step by introducing new surfaces one after the other in an order deduced from the GES according to the procedure described in Section 3.1.2.

For a definite pair of surfaces, the intersection process goes through the following steps:

3. building of an extended restriction of the intersecting surface (F) (cf. Figure 14.d);
 4. intersection of this restriction with the younger surfaces (bounding box B) and building of an extension for the older surface (H) (cf. Figure 14.e);
 5. intersection of the older surface (H) with all the younger ones (F and the bounding box B) (cf. Figure 14.f).
- Stage 6 corresponds to the updating of the topological structure.

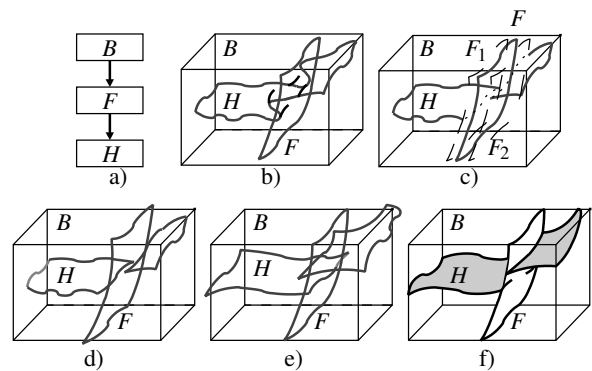


Figure 14: The different stages of the automatic model building illustrated.

3.2.1. Surface extension

Before proceeding to the actual intersection of two surfaces n_i and n_j , one must determine whether these surfaces actually meet or not. To avoid any uncertainties, the parametric surface designated by n_i is at first tangentially extended in the four u, v directions by a distance d' that can be user-chosen (cf. Figure 15).

It is then proceeded to the n_i / n_j intersection, if and only if the two bounding boxes overlap.

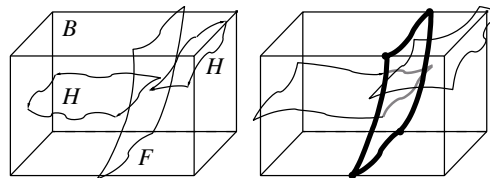


Figure 15: Building of restrictions extension on F and H .

3.2.2. Geometric Intersection

The intersection of n_i and n_j , is operated in the following way:

- intersection of the extent surfaces related to n_i and n_j ; the result is one or several intersection edges, which each have three representations (cf. Figure 16):
 - a curve C_i in the n_i parametric space;

- a curve C_j in the n_j parametric space;
 - a 3D parametric curve C_{3D} .
- in each of the n_i and n_j parametric spaces, intersection of C_i (resp C_j) with the n_i (resp n_j) restriction curves;
 - removal of one portion of the surface n_i or n_j which is interrupted by the other. Assuming that the interrupted surface is n_i , we keep the portion of n_i containing original data.

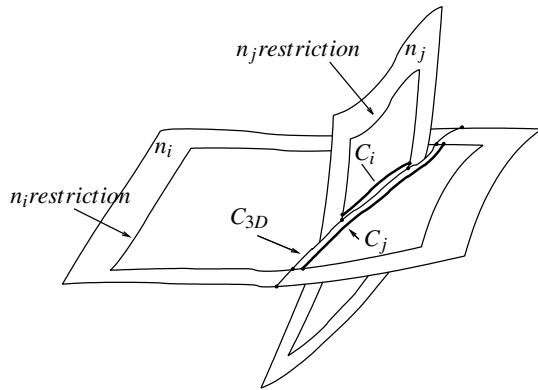


Figure 16: Geometric intersections between surfaces and then between restrictions.

3.2.3. Updating of the G-Map structure

After having performed all the intersections of the geological surfaces corresponding to a node v_i with all the younger surfaces n_j , it is necessary to update the G-Map structure in order to insert the n_i surface itself and all the divisions that n_i has induced on the n_j surfaces in the model. The updated G-Map structure is obtained by refining the new topological faces created by the intersection and by updating their embeddings. This is performed with specific algorithms developed in [Sch02].

3.3. Method using co-refinement of triangulated surfaces

3.3.1. Initial data and pre-processing

This method uses triangulated surfaces that can easily be obtained within the RML package by sampling current parametric surfaces.

When the model to be built only comprises isolated faults (and no fault network), the preprocessing stage only consists in building an incertitude volume around each of them by means of an offset solid, named “pillow structure” in geology (cf. Figure 17). The case of fault networks will be examined hereafter in Section 3.3.3.

3.3.2. Model building

In contrast to the macrotopological methodology, the co-refinement method does not need any outside extension of the intersecting surfaces. The various surfaces are just introduced into the model one after the other in an order corresponding to the downward interpretation course read on the GES (cf. Section 3.1.2).

Each new surface n_i introduced is co-refined with all the n_j surfaces already present in the model. This corefinement consists in computing the intersections between the various triangulated surfaces and in updating the microtopological G-Map model. This is

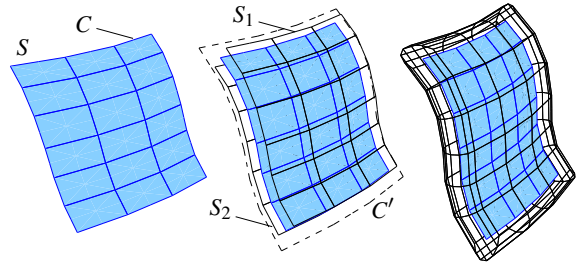


Figure 17: The offset solid is constructed by: building of a given distance d two surfaces S_1 and S_2 parallel to S ; extending S to a contour C' drawn at distance d from the contour C of S ; closing the offset solid along C' .

performed by means of optimized algorithms developed by Nicolas Guiard at University of Poitiers and Ecole des Mines de Paris. This algorithm uses a propagation approach and has thus a complexity of $O(n)$, with respect to the number n of surfaces present in the model. When the surface considered is not a merely planar one but corresponds to an offset solid, the co-refinement is performed both with the external offset solid and with the original planar fault surface.

When the co-refinement procedure is achieved, there is still to remove the portions of the surfaces which no longer belong to the model. This is done by considering the n_j surfaces one after the other, in an order corresponding to the upward intersection course read on the GES (cf. Section 3.1.2) and by removing in each case one portion of the surfaces n_i or n_j which is interrupted by the other.

3.3.3. Building of fault networks

When the model to be built not only comprises individual faults, but one or several fault networks, the model building procedure must be slightly modified. It then goes through the following steps:

- building of an offset solid around each fault of the network;
- co-refinement of all the offset solids corresponding to one definite network;
- removal of the parts of the offset solids, which do not belong to the model; the parts to be removed are determined by examining on the GES, which faults stop on another.

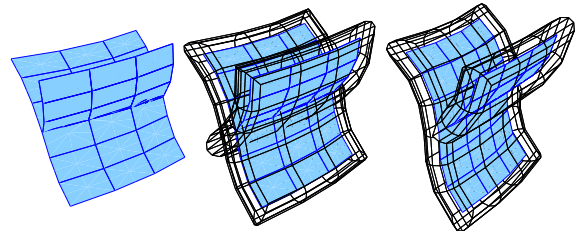


Figure 18: The offset solid built around a fault network.

The result of the above operation is a volumic fault network consisting in an assemblage of offset solids inside which individual planar faults are kept just as in the case of individual offset solids (cf. Figure 18). The volumic fault networks that have been built are then introduced into the model and treated in accordance with the procedure described in Section 3.3.2 in the same way as individual faults.

4. Results

As examples, we will show here models built from two sets of initial data.

The first data set (DS1) concerns tomographic data resulting from experiments operated on the analogical simulator of Institut Français du Pétrole [BPRS01]. They consist in:

- two parallel POL surfaces corresponding to limits of sedimentary formations;
- five TEC surfaces corresponding to faults stopping on one another, which cut out the POL surfaces in different patches shifted with respect to each others.

An unconformable surface posterior to the faults has been added to the original data in order to produce a model showing an erosion configuration. In this example, all the faults either stop on another or cross the entire model. The DS1 data have been interpreted using the two above described methodologies.

The GES corresponding to this geology is shown on Figure 19. Figure 23 shows the results obtained by operating with the macrotopological approach; Figure 20 and Figure 24.a show a result obtained with the microtopological approach.

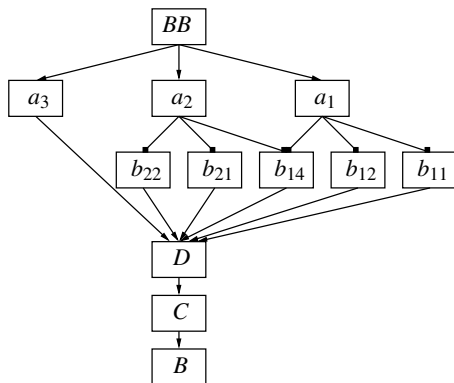


Figure 19: Geological Evolution Scheme.

Figure 23.a represents the rough input data and Figure 23.b the same data after the preprocessing stage, which has divided the two POL surfaces into elementary patches. Figure 23.c corresponds to the resulting consistent geological model showing the five fault surfaces correctly stopping on each others in accordance to the GES specifications and exactly interrupting the two POL surfaces. It is possible to interactively point out geological blocks (cf. Figure 23.d).

The model can also be revised in the case of changes in the geological interpretation. Figure 23.e shows the results obtained by modifying the GES as shown on Figure 21. The new GES specifies that faults a_1 and a_2 , which previously interrupted b_{14} , are now interrupted by b_{14} . After having modified the GES, the result is obtained in this case too, by running again the building of the model starting from the modified elements. Figure 23.e and Figure 23.f show that the change in the GES has induced severe modifications in the topology. Particularly, the shape of the bloc on Figure 23.f differs near the fault on the middle of the scene. This is an outstanding result, the method that we propose being the only which

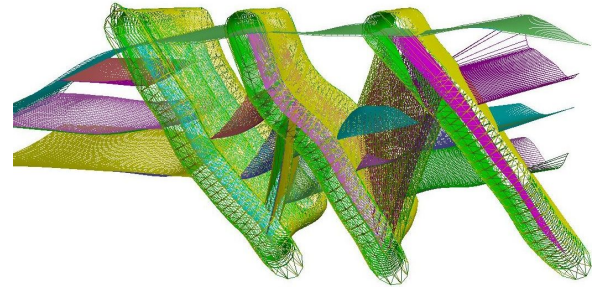


Figure 20: Wireframe view of the final model (DS1) built using the microtopological approach.

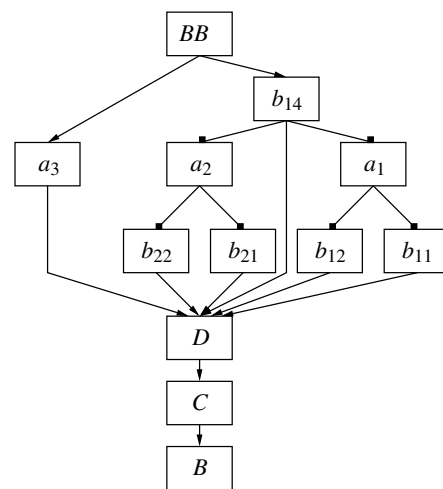


Figure 21: Modified Geological Evolution Scheme.

allows to automatically take into account such 3D topological modifications.

The computing time of the full model DS1, initial geology, using a macrotopological approach, is 190 seconds on a PC Intel Pentium IV 2.6 GHz with 1 GB of RAM. The computing time of the same model, using a microtopological approach, is reduced to 150 seconds on a PC AMD Athlon XP 1800+ with 512 MB of RAM.

The second set of data (DS2) corresponds to surfaces reconstructed starting from a series of parallel cross-sections cut into a seismic cube. The geology consists in two subhorizontal, parallel stratigraphic surfaces and in vertical faults either isolated or parts of a network. In this example, some faults stop inside geological blocks so that some branches of the fault network lie in an hanging position. For this reason, the DS2 data set is fit to be tested using the co-refinement methodology. The results corresponding to this second set of data are represented on Figure 22 and Figure 24.b. As it can be seen, the method provides a correct representation of hanging faults. The computing time for this last model is 88 seconds on a PC AMD Athlon XP 1800+ with 512 MB of RAM.

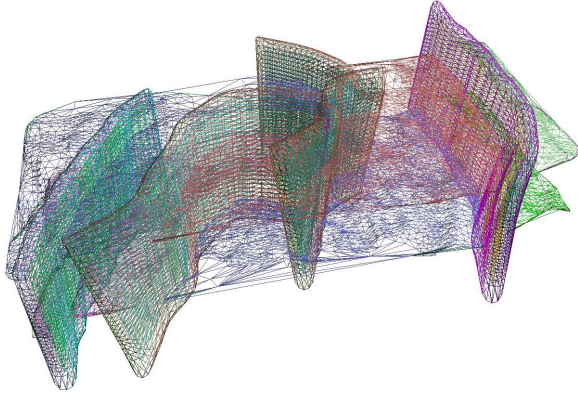


Figure 22: Wireframe view of the final model (DS2) built using the microtopological approach.

5. Further work and conclusion

5.1. Further work

We plan to bring significant improvements to the prototype presented.

As we have seen, the choice of the microtopological approach will also contribute drastically reducing the computing time. In view of the promising results provided by the microtopological approach, this methodology will be chosen for the final version of the prototype. This will enable the user to build any type of models and to produce for a given geology different models possibly showing contrasted topologies in order to take into account geometrical uncertainties or various interpretations.

We further intend to produce a geological pilot package that will comprise 4 different modules:

- a **G3 Server** using for file input/output the RESCUE [webd] exchange format which is a standard for the profession; this server will be able to be coupled to most modelers currently used in gas and oil exploration and will be used to import/export surfaces and models;
- a **Geological Knowledge Editor**, a user friendly interface, which will enable the end user to enter the various surfaces to be processed and to build at the same time the GES which records his/her interpretation;
- a **Pilot**, which will be able to read the GES and to send instructions to a **Co-refinement Processor**.

This last module will itself be in charge of operating the co-refinement procedures and to export consistent geological models to the **G3 Server**.

5.2. Conclusion

We have presented here the prototype of a geological pilot that it will be possible to couple to common geological modelers. This pilot enables the automatic building of a 3D geological model starting from elementary unsegmented surfaces. The result is a fully consistent model both topologically and geologically, which can be easily revised in case of changes of the data and/or of the interpretation made by the user. Improvements are already being studied that will

make this tool an efficient auxiliary for exploration geologists by enabling them to operate the building and updating of voluminous 3D geological models entirely by themselves.

The present work gives a new example of the possibilities offered by 3-G-Maps for monitoring topologies at all stages of the model building. Moreover 3-G-Maps appear as a very flexible tool that can easily be enriched by introducing extra links in order to enable new operations between objects. In the prototype presented, 3-G-Maps do not only help providing correct topologies, they also enable an automatic display of purely geological features such as the belonging of several geological blocks to one geological formation.

This work provides an example of the benefit which can be obtained from a close cooperation between computer graphic specialists and professionals involved in a given application field. It has been possible to take advantage of the specific structure of geological objects to facilitate the model building and to improve the quality of the result by providing models whose geology is fully documented and consistent.

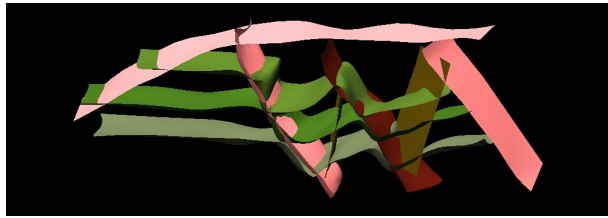
Acknowledgements

This work has been partly supported by the French ministry of industry (FSH). The University of Strasbourg (LSIIT), Lyon I (LIGIM) and the Ecole des Mines de Saint-Etienne (LISSE) also provided significant means at the service of the research presented. We thank our colleagues from IFP, BEICIP FRANLAB, Geomath, Ecole des Mines de Paris, Universities of Poitiers, Strasbourg, Lyon I and from SINTEF (Norway) for useful discussions and propositions.

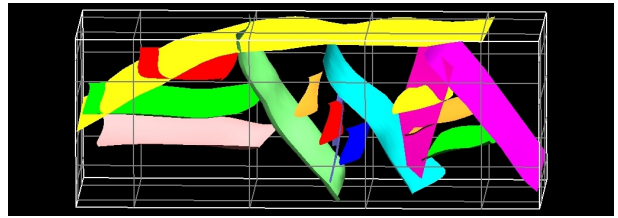
References

- [BDFL93] BERTRAND Y., DUFOURD J., FRANÇON J., LIENHARDT P.: Algebraic specification and development in geometric modeling. *Proc. of TAPSOFT'93* (April 1993). 4
- [BHB03] BRANDEL S., HAEFELE M., BECHMANN D.: A geological application in immersive virtual environments. *VRIC 2003 5th Virtual Reality International Conference* (May 2003). 5
- [BPRS01] BRANDEL S., PERRIN M., RAINAUD J., SCHNEIDER S.: Geological interpretation makes earth models easier to build. *EAGE 63rd Conference, Extended Abstracts I* (June 2001). 3, 6, 8
- [CD96a] CAZIER D., DUFOURD J.-F.: Dérivation de systèmes de réécriture pour construire efficacement des subdivisions planes. *Journées du GDR-PRC de Programmation* (1996). 6
- [CD96b] CAZIER D., DUFOURD J.-F.: opérations booléennes robustes définies sous forme de systèmes de réécriture. *Journées de l'AFIG* (1996). 6
- [FHHR98] FLOATER M., HALBWACHS Y., HJELLE O., REIMERS M.: Omega: A cad-based approach to geological modelling. *Modelling 98 Conference* (June 1998). 1, 2

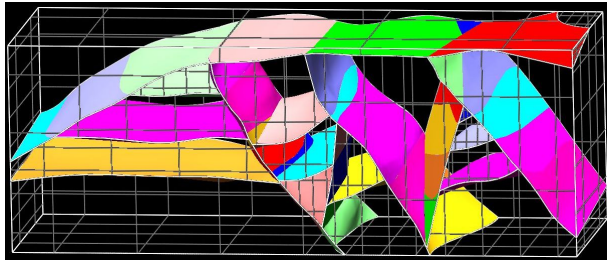
- [HH00] HALBWACHS Y., HJELLE O.: Generalized maps in geological modeling: Object-oriented design of topological kernels. *Advances in Software Tools for Scientific Computing* 10, 1 (2000), 339–356. 4
- [HMW76] HOBBS B., MEANS W., WILLIAMS P.: *An Outline of Structural Geology*. Wiley and sons, 1976. 1
- [Lie89] LIENHARDT P.: Subdivision of n-dimensional spaces and n-dimensional generalized maps. In *5th ACM Symposium on Computational Geometry* (1989), 228–236. 2, 4
- [Lie94] LIENHARDT P.: N-dimensional generalized combinatorial maps and cellular quasi-manifolds. *Journal of Computational Geometry and Applications* 4, 3 (1994), 275–324. 2, 4
- [Mal89] MALLET J.-L.: Discrete smooth interpolation in geometric modeling. *ACM-Transactions on Graphics* 8, 2 (1989), 121–144. 1
- [Mal92] MALLET J.-L.: Gocad: a computer-aided design program for geological applications. *Three-Dimensional Modeling with Geoscientific Information Systems 354* (1992), 123–142. 1
- [Mal02] MALLET J.-L.: *Geomodeling*. Oxford University Press, 2002. 1
- [Per98] PERRIN M.: Geological consistency: an opportunity for safe surface assembly and quick model exploration. *3D Modeling of Natural Objects, A Challenge for the 2000's* 3, 4-5 (June 1998). 2
- [Sch02] SCHNEIDER S.: *Pilotage automatique de la construction de modèles géologiques surfaciques*. PhD thesis, Université Jean Monnet and Ecole des Mines de Saint-Etienne, 2002. 6, 7
- [weba] WEBSITE: The beicip web site. World Wide Web document at <http://www.beicip.com/>. 1, 2
- [webb] WEBSITE: The cas.cade web site. World Wide Web document at <http://www.opencascade.org/>. 5
- [webc] WEBSITE: The earthvision web site. World Wide Web document at <http://www.dgi.com/>. 1
- [webd] WEBSITE: The file exchange format rescue. World Wide Web document at <http://www.posc.org/rescue/>. 9
- [webe] WEBSITE: The gocad web site. World Wide Web document at <http://www.gocad.com/>. 1
- [webf] WEBSITE: The landmark web site. World Wide Web document at <http://www.lgc.com/>. 1



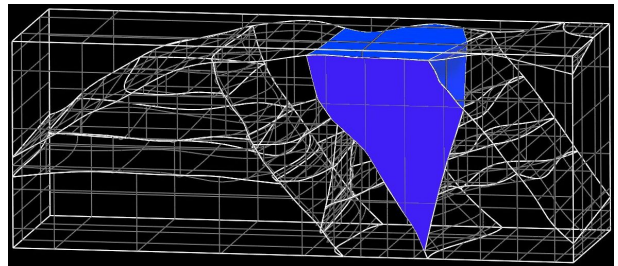
a) raw data



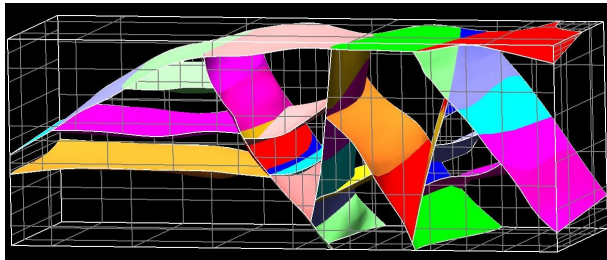
b) initial geology: results after the pre-processing stage



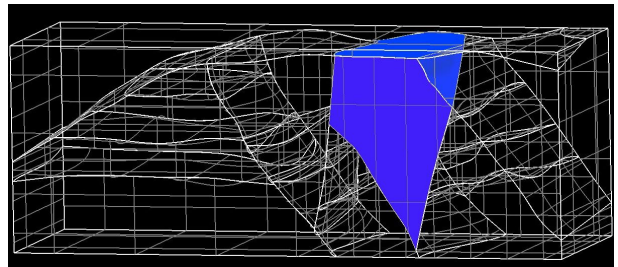
c) initial geology: final model



d) initial geology: view of a geological block

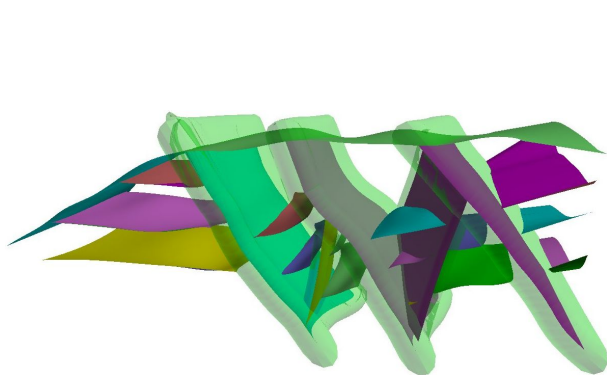


e) modified geology: final model

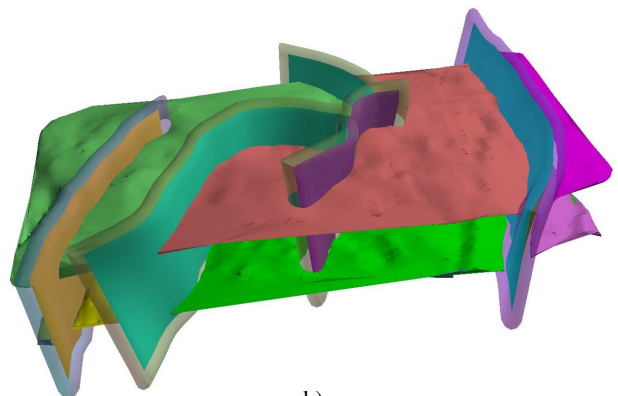


f) modified geology: view of a geological block; the shape of the geological block on (d) appears modified

Figure 23: Macrotopological approach with data set 1.



a)



b)

Figure 24: Microtopological approach with a) data set 1 (initial geology), and b) data set 2: final models.